 ©2007 Kvantovaya Elektronika and Turpion Ltd

LASER SPECTROSCOPY

PACS numbers: 42.62.Fi; 42.55.Rz
DOI: 10.1070/QE2007v037n11ABEH013497

Intracavity laser spectroscopy by using a Fe^{2+} : ZnSe laser

V.A. Akimov, A.A. Voronov, V.I. Kozlovsky, Yu.V. Korostelin, A.I. Landman, Yu.P. Podmar'kov, M.P. Frolov

***Abstract*. A Fe^{2+} : ZnSe laser emitting in the spectral range between 3.77 and 5.05 μm is used for the first time for intracavity laser spectroscopy. The intracavity absorption spectra of methane in the 4.1-μm region are recorded at different instants of lasing (0 – 80 μs) and the dynamics of spectral holes during lasing is investigated. It is found that an intracavity absorption signal linearly increases with time during lasing in the time range from 0 to 80 μs, which provides the effective absorption length up to 24 km.**

Keywords: *intracavity laser spectroscopy, Fe^{2+} : ZnSe laser, IR lasers, solid-state lasers.*

1. Introduction

At present the II – VI crystals doped with bivalent transition-metal ions attract considerable interest [1 – 4]. This is explained by a number of reasons.

First, recently an increasing demand is observed for low-cost and compact mid-IR lasers for a variety of applications such as the environment monitoring, control of technological processes, eye-safe laser location, analysis of gas impurities at low concentrations, noninvasive methods of medical diagnostics with the help of eye-safe lasers, optical communication, spectroscopic studies, etc. The II – VI crystals doped with transition-metal ions form a class of new promising laser media emitting in the spectral region from 2 to 5 μm [1]. In particular, efficient lasing and continuous wavelength tuning of the output radiation was obtained in Fe^{2+} : ZnSe crystals in the spectral region from 3.77 to 5.05 μm [5 – 8]. Because this range contains the transparency window of the atmospheric air located near 4 μm, Fe^{2+} : ZnSe lasers are also promising for the remote sensing of the atmosphere.

Second, the search is continuously pursued for new solid saturable absorbers that could be used as passive Q switches to generate giant pulses in mid-IR lasers. The generation of giant pulses considerably extends the possibilities of the laser and is required in a number of practical problems. The Fe^{2+} : ZnSe crystals can be used as convenient saturable absorbers for lasers emitting in the 3-μm range, which was demonstrated by the passive Q-switching of the Er : YAG [9] and Er : Cr : YSGG lasers [10] emitting at 2.94 and 2.8 μm, respectively.

This paper is devoted to the study of a new field of possible applications of a Fe^{2+} : ZnSe laser. We investigated the principal possibility of using this laser in the method of intracavity laser spectroscopy (ICLS) [11] for the highly sensitive detection of weak absorption lines in the mid-IR spectral range. The pronounced tendency to extend the range of spectral studies to the IR region, which is typical for most of the highly sensitive laser absorption methods, is caused by the intention to obtain lower detection thresholds for gases having relatively strong IR absorption lines related to vibrational transitions.

In the ICLS method, broadband lasers are used, in which the homogeneous width of the amplification band of the active medium is large compared to the absorption linewidth of an intracavity gas under study. In particular, the II – VI crystal doped with transition-metal ions satisfy this requirement. It was shown in papers [12 – 14] that a Cr^{2+} : ZnSe laser can be used for ICLS in the spectral region from 2.1 to 3.1 μm. It seems that a Cr^{2+} : ZnSe crystal provided so far the longest-wavelength generation in the ICLS method. The use of Fe^{2+} : ZnSe crystals emitting in the spectral region from 3.77 to 5.05 μm provides a further extension of the spectral range of ICLS to the IR region.

2. Experimental setup and methods for studying the spectral dynamics of a Fe^{2+} : ZnSe laser

We studied the spectral radiation dynamics of a multimode (broadband) Fe^{2+} : ZnSe laser in the presence of narrowband intracavity losses caused by absorption lines of methane. The optical scheme of the setup is presented in Fig. 1.

The Fe^{2+} : ZnSe laser was pumped at 2.94 μm by a flashlamp-pumped free-running Er : YAG laser emitting 120-μs, 190-mJ pulses with a repetition rate of 0.5 Hz. The laser pulse energy was measured with a Solo-X calorimeter with a QE12LP-S-MB-DO pyroelectric head. Curve (*1*) in Fig. 2 shows the oscillogram of a pump pulse recorded with photodetector P1 (PD36-03 photodiode) and a Tektronix TDS3052B oscilloscope. The pump radiation was linearly polarised to minimise its loss on elements of the

V.A. Akimov, A.A. Voronov Moscow Institute of Physics and Technology (State University), Institutskii per. 9, 141700 Dolgoprudnyi, Moscow region, Russia;
V.I. Kozlovsky, Yu.V. Korostelin, A.I. Landman, Yu.P. Podmar'kov, M.P. Frolov P.N. Lebedev Physics Institute, Russian Academy of Sciences, Leninsky prosp. 53, 119991 Moscow, Russia;
e-mail: frolovmp@x4u.lebedev.ru

Received 13 December 2006; revision received 8 May 2007
Kvantovaya Elektronika **37** (11) 1071 – 1075 (2007)
Translated by M.N. Sapozhnikov

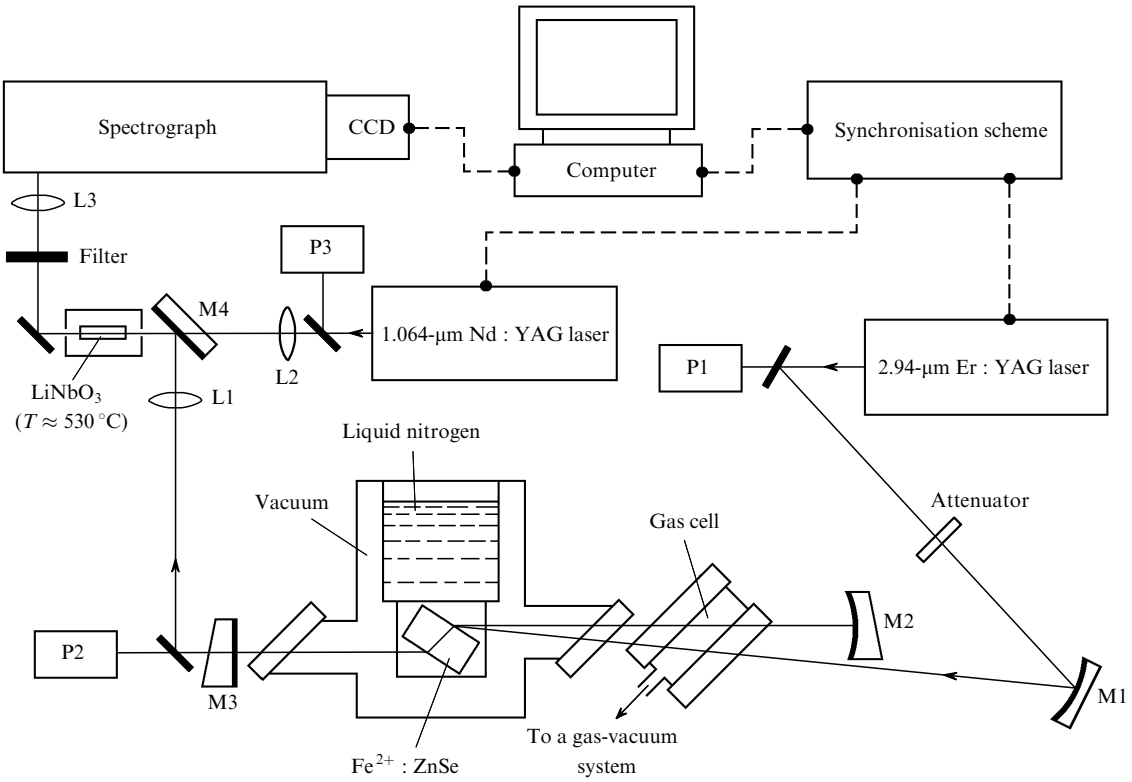

Figure 1. Scheme of the experimental setup.

Fe^{2+} : ZnSe laser cavity oriented at the Brewster angle. The pump energy was controlled with calibrated optical filters. The pump beam was directed into the Fe^{2+} : ZnSe crystal by focusing mirror M1 with the radius of curvature 50 cm. The pump spot in front of the crystal had the shape of an ellipse with axes 1.2 and 1 mm elongated along the vertical direction. The pump radiation was incident on the crystal at an angle of $\sim 3^\circ$ to the optical axis of the cavity.

The 10-mm-thick active element of the Fe^{2+} : ZnSe laser of transverse size 17×10 mm was cut from a Fe^{2+} : ZnSe single crystal grown from a vapour phase on a single-crystal seed by using the chemical transport in hydrogen and doped directly during growing. The concentration of Fe^{2+} ions, measured from the absorption spectrum by using the absorption cross section presented in [5], was $\sim 1 \times 10^{18}$ cm^{-3}. The active element was mounted in the cavity at the Brewster angle.

Lasing in a Fe^{2+} : ZnSe crystal occurs between the $^5T_2$ and ^5E states of the Fe^{2+} ion. The lifetime of the upper $^5T_2$ laser level of the Fe^{2+} ion in the ZnSe matrix decreases with increasing temperature from 105 μs at 120 K to 5 μs at 220 K [5] due to the increase in the rate of nonradiative relaxation and is equal to 355 ns at room temperature [7]. This requires the cooling of the Fe^{2+} : ZnSe crystal to obtain lasing upon pumping by long pulses. For this reason, the active element in our setup was mounted on a cold copper finger inside a cryostat cooled with nitrogen down to 85 K. The cryostat windows were made of plane–parallel CaF_2 plates mounted at the Brewster angle.

The Fe^{2+} : ZnSe laser cavity was formed by rear aluminium spherical mirror M2 with the radius of curvature 50 cm and plane output mirror M3 with the transmission coefficient 0.5% at the laser wavelength, which was deposited on a CaF_2 wedge-like substrate (the wedge angle was 5°) to eliminate interference effects. The optical length of the cavity L_c was 33 cm. A 1.5-cm-thick gas cell with CaF_2 windows was mounted inside the cavity. The cell was connected with a gas-vacuum system for cell evacuating and filling with absorbing gases. The cell was oriented at the Brewster angle and therefore the laser radiation was absorbed in the gas under study at the length 2.5 cm during each passage in the cell.

The output energy of the Fe^{2+} : ZnSe laser pumped by 90 mJ was 2 mJ. Laser pulses of duration 80–100 μs, depending on the pump energy, were detected with photodetector P2 (FSG-22 photoresistor) [curve (*2*) in Fig. 2]. The lasing spectrum had a maximum at 4.1 μm.

The emission spectrum of the Fe^{2+} : ZnSe laser and its spectral dynamics were studied by up-converting the broad-

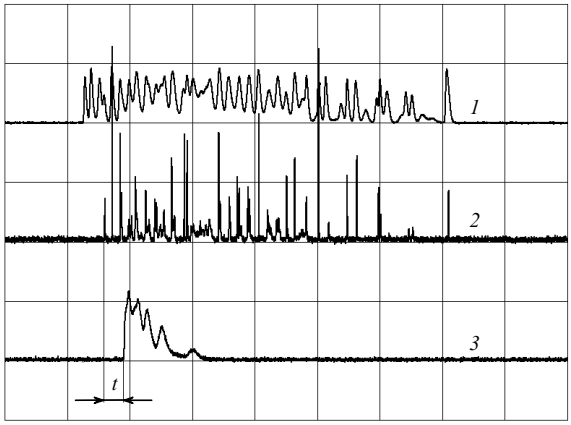

Figure 2. Oscillograms of the pump (*1*), Fe^{2+} : ZnSe (*2*) and Nd : YAG (*3*) laser pulses. The sweep speed is 20 μs div^{-1}.

band IR laser radiation to the shorter-wavelength radiation at 0.84 μm due to the sum-frequency generation by mixing the IR radiation in a $LiNbO_3$ nonlinear crystal (temperature tuned 90° phase matching) with the narrowband 1.064-μm radiation from a Nd : YAG laser (the measured linewidth did not exceed 0.04 cm^{-1} and was determined by the spectrograph resolution) emitting pulses of shorter duration than those of the Fe^{2+} : ZnSe laser. We used this method for recording IR spectra earlier for measuring intracavity absorption spectra by using $Co^{2+} : MgF_2$ [15] and Cr^{2+} : ZnSe [12, 13] lasers. Figure 2 [curve (*3*)] shows the oscillogram of the Nd : YAG laser pulse recorded with photodetector P3 (FD-10 photodiode). The output energy of the Nd : YAG laser was 5 mJ.

To provide phase matching, the $LiNbO_3$ crystal was heated up to $\sim 530\,^{\circ}C$. The beams from Fe^{2+} : ZnSe and Nd : YAG lasers were focused and made coincident inside the lithium niobate crystal with the help of lenses L1 and L2 and dichroic mirror M4, which had the reflectance close to 100 % at 4.1 μm and was transparent at 1.064 μm. The up-converted radiation was selected with an optical filter and focused by lens L3 on the entrance slit of a diffraction spectrograph (theoretical resolution of 0.043 cm^{-1}) equipped with a CCD array coupled with a PC. A pulse from the Nd : YAG laser could be delayed with respect to the pump laser pulse with the help of a synchronisation scheme, which allowed us to record the emission spectrum of the Fe^{2+} : ZnSe laser at any instant of lasing and to observe the development of intracavity absorption spectra in time. The delay time t was measured from the leading edge of the Fe^{2+} : ZnSe laser pulse to the leading edge of the Nd : YAG laser pulse (Fig. 2).

We used methane for intracavity absorption measurements, which absorbs in the emission region of the Fe^{2+} : ZnSe laser [16]. A gas cell was filled with an air : methane = 100 : 1 mixture at a total pressure of 1 atm.

3. Experimental results and discussion

The emission spectra of the Fe^{2+} : ZnSe laser in the presence of intracavity absorption were recorded for delay times from 0 to 80 μs. The pump energy of the Fe^{2+} : ZnSe laser during the recording of the spectra exceeded the threshold value by 6 – 7 times. Figure 3a and b demonstrate the emission spectra recorded for delay times 20 and 40 μs, respectively. These spectra were recorded after averaging over 100 laser pulses. The holes observed in the spectra are caused by the absorption lines of methane.

We compared the experimental absorption spectra with the model spectra calculated by using the HITRAN database [16]. The numerical simulations were performed taking into account that the effective absorption length L_{eff} in the ICLS method is described by the expression

$$L_{\text{eff}} = ct_{\text{g}}L_{\text{ab}}/L_{\text{c}}, \tag{1}$$

where L_{c} is the optical length of the laser cavity containing the absorbing layer of thickness L_{ab}; t_{g} is the lasing time measured from the instant of achieving the threshold inverse population; and c is the speed of light. In this case, it is necessary keep in mind the following. Because the lifetime of the upper laser level in solid-state lasers is much longer than the lifetime of a photon in the cavity, the first radiation spike appears within the time t_0 after the

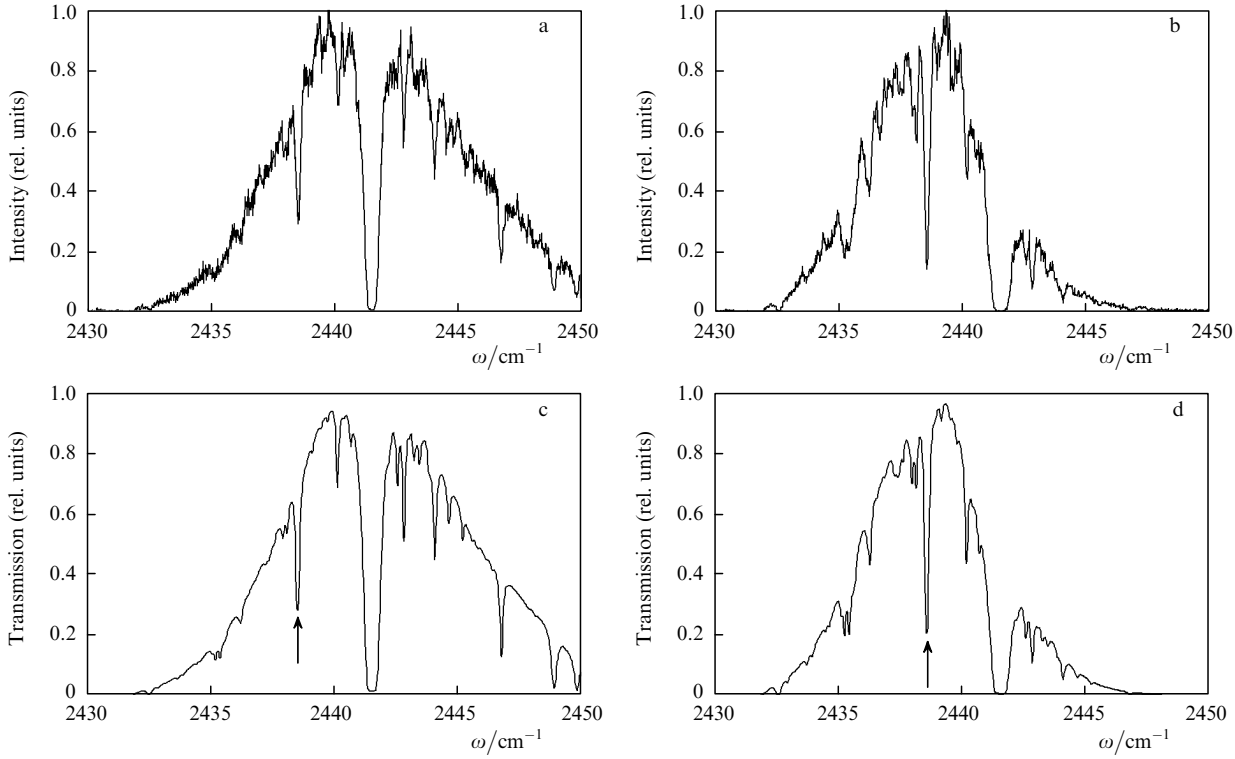

Figure 3. Emission spectra of the Fe^{2+} : ZnSe laser recorded with the time delays 20 (a) and 40 μs (b) when a gas cell was filled with the air : methane = 100 : 1 mixture at a total pressure of 1 atm, and the absorption spectra of the same mixture calculated for absorbing-layer lengths 0.68 (c) and 1.14 km (d) by using the HITRAN database taking into account the envelope of the emission spectrum of the Fe^{2+} : ZnSe laser.

appearance of the inverse population (the cavity build-up time). Therefore, the lasing time used in simulations was written in the form $t_g = t_0 + t$, where the value of t_0 was selected to obtain the best fit with the experimental data. We also assumed in simulations that the instrumental function of the spectrograph had the diffraction profile of width 0.05 cm^{-1}.

Figures 3c and d present the model absorption spectra for the mixture used in experiments, which were calculated taking into account the envelope of the emission spectra of the Fe^{2+} : ZnSe laser for the absorption lengths 0.68 and 1.14 km, respectively. These values are equal to the effective absorption lengths for experimental conditions under which the spectra in Figs 3a and b were obtained. The best fit of the experimental spectra was achieved by using the value $t_0 = 10$ μs in simulations.

Because the delay of the leading edge of the Fe^{2+} : ZnSe laser pulse with respect to the leading edge of the pump Er : YAG laser pulse was approximately 6 μs, the cavity build-up time t_0 could not exceed this value. It seems that the value 10 μs is determined not only by the lasing development time t_0 but also by a rather large duration (FWHM $\sim$ 10 μs) of the Nd : YAG laser pulse and a considerable scatter ($\pm$3 μs) of the delay time t upon averaging spectra.

We studied quantitatively the dynamics of intracavity absorption by analysing the spectral hole at $\omega =$ 2438.56 cm^{-1} shown by the arrow in Figs 3c, d. The hole appears due to absorption of laser radiation by partially overlapping methane lines at frequencies 2438.5109, 2438.5282, and 2438.5885 cm^{-1} [16].

Figure 4 shows the time dependence of the intracavity absorption signal $\ln(I_0/I)$, where I is the laser radiation intensity at the hole centre and I_0 is the intensity of the laser emission spectrum envelope at the hole centre. One can see that the intracavity absorption signal linearly increases with increasing the delay time during the entire laser pulse, which corresponds to the modified Bouguer – Lambert – Beer law describing the spectral dynamics of a multimode laser in the presence of intracavity absorption at frequency ω:

$$I(\omega)/I_0(\omega) = \exp[-k(\omega)L_{\text{eff}}]$$

$$= \exp[-k(\omega)c(t_0 + t)L_{\text{ab}}/L_{\text{c}}]. \quad (2)$$

Here, $I(\omega)$ is the laser radiation intensity at frequency ω; $I_0(\omega)$ is the intensity of the laser emission spectrum envelope at frequency ω; and $k(\omega)$ is the absorption coefficient at frequency ω. The straight line drawn through experimental points has an origin at the point $t = -13$ μs corresponding to $t_0 = 13$ μs, in satisfactory accordance with the value 10 μs found in numerical simulations.

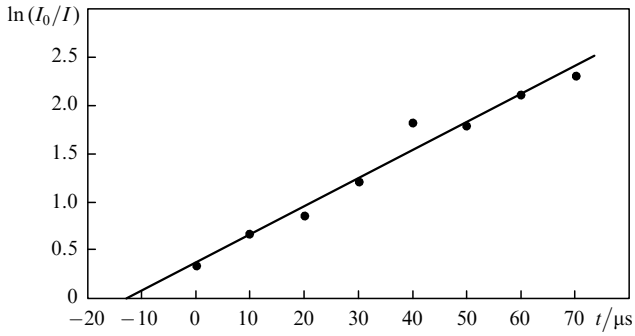

Figure 4. Dependence of the intracavity absorption signal $\ln(I_0/I)$ on the delay time of the Nd : YAG laser pulse with respect to the Fe^{2+} : ZnSe laser pulse.

The filling coefficient $L_{\text{ab}}/L_{\text{c}}$ for the Fe^{2+} : ZnSe laser cavity in our study was 0.076, which was determined by the designs of our cryostat and an absorbing cell, as well as by the geometry of the laser cavity. It is obvious that, by using a compact cryostat and a longer cavity, the coefficient of cavity filling by an absorbing gas can be made close to unity. In this case, the effective absorption length for 80-μs laser pulses will be 24 km. The minimal absorption detected in our spectra was determined by the noise of the laser emission spectrum. As a result, for the maximum laser pulse duration, we could find the absorption lines that produced spectral holes with the relative depth exceeding 25 %. For the effective absorption length equal to 24 km, such holes can be produced by absorption lines with the absorption coefficient exceeding $\sim 10^{-7}$ cm^{-1}.

4. Conclusions

We have used for the first time a Fe^{2+} : ZnSe laser for intracavity laser spectroscopy. This laser extends the spectral region of this method up to 5 μm. A linear increase in the sensitivity of the emission spectrum of the Fe^{2+} : ZnSe laser to intracavity absorption was observed upon increasing the lasing duration up to at least 80 μs, which, in the case of a complete filling of the cavity with absorbing matter, provides the effective absorption length equal to 24 km and allows the detection of weak lines with the absorption coefficient $\sim 10^{-7}$ cm^{-1}. Because no deviation from the linear dependence of an intracavity absorption signal on the lasing time has been observed, the sensitivity of the method can be further increased by increasing the laser pulse duration.

We demonstrated earlier [6] the efficient operation of a Fe^{2+} : ZnSe laser upon cooling its active element down to $\sim$ 220 K by a thermoelectric element. This circumstance and the results obtained in the present paper suggest that the Fe^{2+} : ZnSe laser can be used for the development of a low-cost compact mid-IR intracavity absorption spectrometer.

Acknowledgements. This work was supported by the Russian – American Program 'Fundamental Studies and High Education' of the Ministry of Education and Science of the Russian Federation and the American Civil Research and Development Foundation (Grant No. CRDF MO-011-0/B2M411), the President of the Russian Federation for the Support of Leading Scientific Schools (Grant No. NSh-6055.2006.02), the Program of Fundamental Studies of the Department of Physical Sciences, RAS 'Coherent Optical Radiation of Semiconductor Compounds and Structures', and the Program 'Development of the Scientific Potential of the High School' of the Ministry of Education and Science of the Russian Federation.

References

1. DeLoach L.D., Page R.H., Wilke G.D., Payne S.A., Krupke W.F. *IEEE J. Quantum Electron.*, **32**, 885 (1996).
2. Kuck S. *J. Alloys Compounds*, **341**, 28 (2002).

3. Carrig T.J. *J. Electron. Mater.*, **31**, 759 (2002).
4. Sorokina I.T. *Opt. Mater.*, **26**, 395 (2004).
5. Adams J.J., Bibeau C., Page R.H., Krol D.M., Furu L.H., Payne S.A. *Opt. Lett.*, **24**, 1720 (1999).
6. Voronov A.A., Kozlovsky V.I., Korostelin Yu.V., Landman A.I., Podmar'kov Yu.P., Frolov M.P. *Kvantovaya Elektron.*, **35**, 809 (2005) [*Quantum Electron.*, **35**, 809 (2005)].
7. Akimov V.A., Voronov A.A., Kozlovsky V.I., Korostelin Yu.V., Landman A.I., Podmar'kov Yu.P., Frolov M.P. *Kvantovaya Elektron.*, **36**, 299 (2006) [*Quantum Electron.*, **36**, 299 (2006)].
8. Fedorov V.V., Mirov S.B., Gallian A., Badikov V.V., Frolov M.P., Korostelin Yu.V., Kozlovsky V.I., Landman A.I., Podmar'kov Yu.P., Akimov V.A., Voronov A.A. *IEEE J. Quantum Electron.*, **42**, 907 (2006).
9. Voronov A.A., Kozlovsky V.I., Korostelin Yu.V., Landman A.I., Podmar'kov Yu.P., Poluskin V.G., Frolov M.P. *Kvantovaya Elektron.*, **36**, 1 (2006) [*Quantum Electron.*, **36**, 1 (2006)].
10. Gallian A.R., Martinez A., Marine P., Fedorov V.V., Mirov S.B., Badikov V.V., Boutoussov D.M., Andriasyan M. *Proc. Conf. 'Photonics West, LASE 2007'* (San Jose, California, USA, San Jose Conventional Center) Paper 6451-20.
11. Pakhomycheva L.A., Sviridenkov E.A., Suchkov A.F., Titova L.V., Churilov S.S. *Pis'ma Zh. Eksp. Teor. Fiz.*, **12**, 60 (1970).
12. Akimov V.A., Kozlovsky V.I., Korostelin Yu.V., Landman A.I., Podmar'kov Yu.P., Frolov M.P. *Kvantovaya Elektron.*, **34**, 185 (2004) [*Quantum Electron.*, **34**, 185 (2004)].
13. Akimov V.A., Kozlovsky V.I., Korostelin Yu.V., Landman A.I., Podmar'kov Yu.P., Frolov M.P. *Kvantovaya Elektron.*, **35**, 425 (2005) [*Quantum Electron.*, **35**, 425 (2005)].
14. Picque N., Gueye F., Guelachvili G., Sorokin E., Sorokina I.T. *Opt. Lett.*, **30**, 3410 (2005).
15. Frolov M.P., Podmar'kov Yu.P. *Opt. Commun.*, **155**, 313 (1998).
16. The HITRAN database, 2004 edition (www.hitran.com).